International Journal of Research Publication and Reviews

Journal homepage: www.ijrpr.com ISSN 2582-7421

Transient Thermal Response Mapping in Prismatic Cells Under Pulsed Charging Using Embedded Sensor Arrays

Chimezie Oguike

Department of Mechanical Engineering, University of Cape Town, South Africa

ABSTRACT

Fast charging protocols for lithium-ion batteries have introduced significant thermal challenges, especially for prismatic cell formats used in electric vehicles and grid storage. Understanding transient thermal response during pulsed charging is critical for ensuring safe operation and extending battery life. This study presents a high-resolution thermal characterization technique using embedded sensor arrays within commercial-grade prismatic lithium-ion cells to track real-time heat generation and dissipation patterns under pulsed current profiles. Cells were charged using intermittent high-current pulses (up to 4C) with rest periods, emulating real-world fast-charging scenarios. Thermocouple and thin-film thermistor arrays were strategically embedded between electrode layers and beneath cell tabs to capture localized temperature variations. Results showed rapid thermal spikes exceeding 50°C within milliseconds of current onset, followed by non-linear cooling curves, highlighting thermal inertia in cell construction. The spatiotemporal temperature data was further used to derive effective thermal conductivity and to calibrate a multi-layered lumped thermal model of the prismatic structure. Insights revealed poor heat dispersion near tab areas and asymmetrical thermal gradients, emphasizing the need for improved tab cooling and internal layout optimization. This approach allows for predictive diagnostics, as recurring thermal anomalies were found to align with early signs of localized impedance growth and lithium plating. The methodology is applicable for validating battery thermal models and for benchmarking various cell designs under rapid charging conditions. By incorporating thermal sensors directly within cells, the study demonstrates a new standard for internal temperature profiling that enables safer and more efficient energy storage systems.

Keywords: Prismatic Cells, Pulsed Charging, Embedded Sensors, Thermal Response, Lithium Plating, Battery Safety

1. INTRODUCTION

1.1. Background and Motivation

The rapid evolution of energy storage systems has placed lithium-ion batteries (LIBs) at the center of global electrification efforts. Their high energy density, low self-discharge rate, and relatively long cycle life have made them essential in applications ranging from consumer electronics to electric vehicles (EVs). Among the various formats, prismatic lithium-ion cells are increasingly favored in electric mobility and grid storage due to their compact packaging, efficient heat dissipation geometry, and structural compatibility with module enclosures [1].

Despite these advantages, lithium-ion cells are prone to thermal stress during fast charging and discharging, which compromises their performance, safety, and lifespan. In the worst-case scenarios, thermal runaway—a chain reaction triggered by excessive internal heat—can cause fire or explosion. In real-world scenarios, temperature non-uniformity within the cell architecture often accelerates material degradation and reduces reliability [2]. Prismatic cells, in particular, with their layered architecture and high-capacity design, are vulnerable to such internal gradients. Therefore, a deeper understanding of the transient thermal behavior of prismatic cells under operational stress is crucial for predictive control and risk mitigation.

In conventional battery management systems (BMS), surface-mounted thermocouples provide macroscopic temperature data but lack the spatial resolution to map internal behavior. Consequently, the industry demands a more granular understanding of temperature evolution inside the cell to refine thermal models and improve design algorithms [3].

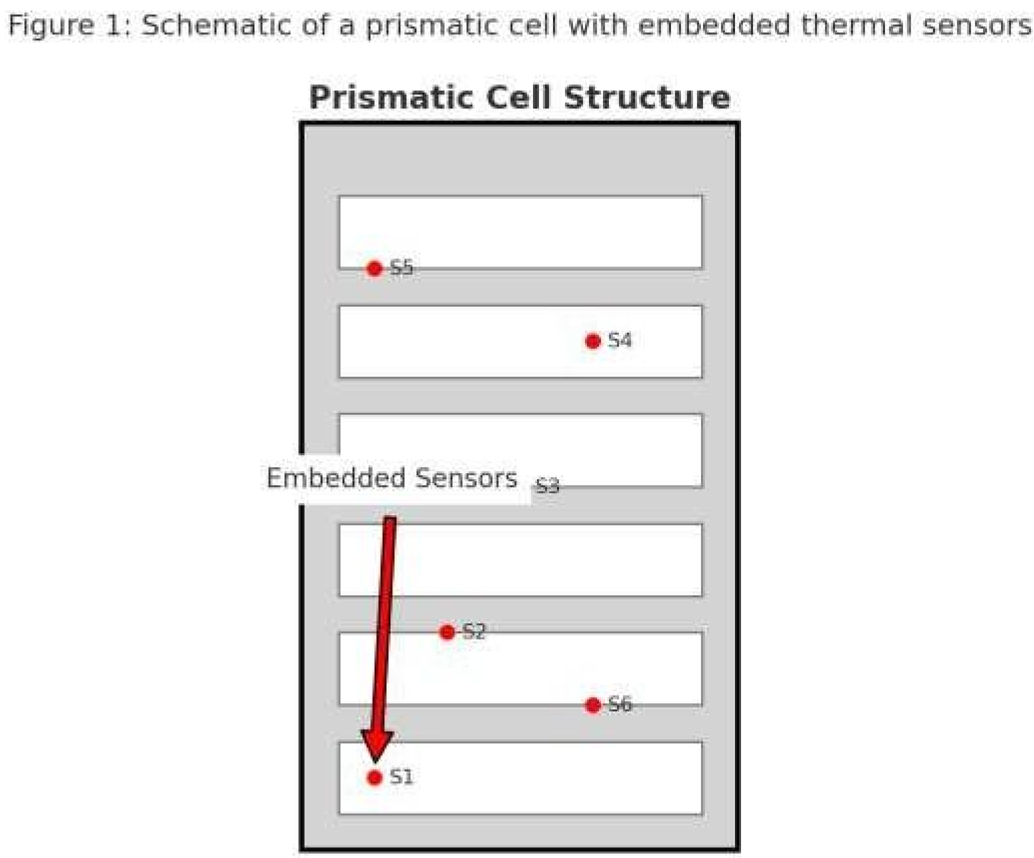

Figure 1: *Schematic of a prismatic cell with embedded thermal sensors*

1.2. Importance of Thermal Management in Prismatic Cells

Thermal management in prismatic cells extends beyond safety—it influences energy efficiency, cycle life, and state-of-charge accuracy. The internal resistance of a lithium-ion cell, which is temperature-dependent, affects charge transfer kinetics and electrochemical stability. For prismatic cells with high volumetric energy density, local hotspots often form due to uneven current distribution, passive layer growth, and heat entrapment near electrodes [4].

These hotspots may not always be reflected at the surface, leading to false thermal assessments by external sensors. As a result, systems relying solely on surface data might either undercool, risking degradation, or overcool, reducing efficiency. An optimized thermal design must thus consider internal gradients and not just external manifestations [5].

Furthermore, prismatic cells are often tightly packed in modules with limited airflow, increasing the risk of heat accumulation. This makes the early identification of internal thermal rise essential in preemptive control strategies. A key research priority has therefore emerged: developing embedded diagnostic tools capable of offering real-time, spatially resolved insights into thermal evolution under dynamic operating conditions.

1.3. Relevance of Pulsed Charging Techniques

Conventional constant current (CC) or constant voltage (CV) charging strategies, while simple to implement, often induce steady-state heat accumulation, which leads to suboptimal thermal profiles. Pulsed charging, in contrast, has emerged as a promising alternative, offering both performance and thermal management advantages [6].

In pulsed charging, the input current is periodically interrupted, creating intervals that allow partial heat dissipation and ion redistribution within the electrolyte. These rest periods not only reduce average cell temperature but also limit lithium plating, a major cause of cell aging and failure. The dynamic response of a cell to pulsed input, especially in terms of thermal inertia, provides a unique window into the internal heat generation mechanisms [7].

However, understanding the thermal effects of these pulse profiles in real time remains a challenge. Traditional methods cannot capture the sub-second fluctuations and localized heat zones that occur during pulse transitions. This underscores the need for real-time, embedded thermal diagnostics tailored to monitor the impact of pulsed charging protocols on thermal dynamics.

1.4. Advantages of Embedded Sensor Arrays for Thermal Diagnostics

The application of embedded sensor arrays within lithium-ion batteries marks a significant leap in battery diagnostics. Unlike external sensors, embedded arrays can capture transient, spatially resolved thermal data from various internal layers, including electrodes, separators, and electrolyte regions [8]. These arrays typically consist of high-precision thermocouples, resistance temperature detectors (RTDs), or microelectromechanical system (MEMS) sensors that are designed to function under high electrochemical stress.

The spatial arrangement of sensors enables the creation of thermal maps during charging and discharging events. This is especially relevant in prismatic cells, where edge-to-core temperature gradients are often significant but not externally detectable. These maps facilitate the validation of electro-thermal models and provide ground-truth data for simulation tools.

Furthermore, embedded arrays support closed-loop thermal control, wherein real-time data can be used to trigger localized cooling or dynamic charging adjustments. They also offer invaluable insights into material behavior, thermal lag, and delayed heat propagation, which are often missed in conventional BMS configurations [9].

Such insights are particularly important when testing novel charging strategies or under high-power applications where the rate of heat generation varies rapidly. Embedded diagnostics thus not only enhance safety and performance but also contribute to design optimization at both the cell and system levels.

1.5. Study Objective and Scope

This study aims to investigate the transient thermal response of prismatic lithium-ion cells subjected to pulsed charging profiles using embedded thermal sensor arrays. By integrating multiple sensors within the cell structure, we aim to map internal temperature distributions in real time, identify critical thermal patterns, and correlate these with pulse parameters and cell geometry.

Specifically, the research seeks to:

- Quantify the effect of pulse width, duty cycle, and current amplitude on internal temperature evolution;
- Detect hotspot formation zones and their temporal dynamics;
- Validate the feasibility and accuracy of embedded sensor arrays in capturing meaningful thermal signatures under realistic charging conditions [10].

The study is constrained to a specific prismatic cell chemistry (Nickel Manganese Cobalt, NMC) and a limited set of pulse protocols designed to simulate aggressive yet realistic EV charging conditions. All testing is conducted under controlled thermal and environmental settings to minimize external influences.

Ultimately, the goal is to provide a foundational understanding that could inform future thermal management strategies and BMS integration practices, especially as battery technologies evolve toward faster, denser, and safer energy storage solutions.

2. LITERATURE REVIEW AND THEORETICAL BACKGROUND

2.1. Thermal Behavior in Lithium-ion Prismatic Cells

2.1.1. Heat Generation Mechanisms

In lithium-ion prismatic cells, heat generation is a multifaceted process driven by both reversible and irreversible phenomena. During charging and discharging, resistive heating—primarily due to internal ohmic losses in electrodes, electrolyte, and current collectors—constitutes a significant fraction of the total heat [6]. This is often referred to as Joule heating, which increases with internal resistance and current intensity. In addition, entropy changes resulting from the intercalation and deintercalation of lithium ions contribute to reversible heat generation or absorption, depending on the state of charge.

Irreversible side reactions, such as solid electrolyte interphase (SEI) growth or lithium plating at the anode during high-rate charging, further exacerbate localized heating. These exothermic reactions, while not dominant under nominal conditions, become critical under high loads or elevated temperatures [7]. Understanding the balance between these processes is key to modeling and managing heat evolution in real-world battery usage.

2.1.2. Anisotropic Thermal Properties

Prismatic cells exhibit directionally dependent thermal properties, primarily due to their layered construction. The in-plane thermal conductivity, often dominated by the metallic current collectors, is significantly higher than the through-plane conductivity governed by the porous electrodes and separator [8]. This anisotropy means heat tends to spread laterally rather than vertically, contributing to uneven thermal fields—particularly under rapid pulsed charging where local gradients develop quickly.

As the cell's internal structure governs the thermal pathways, any inconsistency in electrode alignment, compression, or layer thickness can produce asymmetric thermal responses, which further complicates predictive modeling [9]. Identifying and quantifying this behavior is crucial for real-time control and adaptive cooling mechanisms.

2.1.3. Heat Dissipation Pathways

Heat dissipation in prismatic cells relies on conduction, convection, and, to a lesser extent, radiation. The primary pathway is through conduction from the internal layers to the cell casing and subsequently to the external cooling system. However, cell packaging, module density, and thermal interface materials significantly affect this process [10].

The use of compact packs in electric vehicles limits airflow and convective dissipation, making conduction efficiency a bottleneck. Moreover, the outermost surfaces of prismatic cells often exhibit lower thermal resistance compared to internal core zones, leading to thermal bottlenecks and hidden hotspots. Addressing these inefficiencies requires not only advanced cooling architectures but also deeper insight into heat generation sites within the cell.

2.2. Pulsed Charging Techniques and Thermal Impacts

2.2.1. Concept and Implementation of Pulsed Charging

Pulsed charging involves applying intermittent bursts of current rather than a continuous charging stream. A typical cycle comprises a high-current pulse followed by a rest or relaxation phase, allowing internal ions to redistribute and partial thermal dissipation to occur [11]. This method not only minimizes overall heat generation but also helps reduce polarization losses during the inter-pulse intervals.

Implementation of pulsed charging requires synchronized control of current amplitude, duty cycle, and pulse width. These parameters are often tailored to battery chemistry and thermal constraints. For example, shorter pulse durations at higher currents may be used to improve fast charging while maintaining acceptable thermal levels [12]. However, this approach demands precise thermal feedback to prevent cumulative heat buildup and mechanical stress.

2.2.2. Impact on Thermal and Electrochemical Behavior

From a thermal perspective, pulsed charging offers the advantage of cyclical heat relaxation, which interrupts the continuous rise in temperature seen in conventional charging. This often leads to a more uniform and stable internal temperature profile, especially in high-density cells like prismatic formats [13]. The relaxation periods give the thermal mass time to redistribute heat, lowering the risk of localized overheating.

Electrochemically, pulsed regimes improve lithium-ion diffusion, reducing the likelihood of plating and increasing the effective rate capability of the cell. However, the switching dynamics of pulsed systems can introduce transient electrochemical states that complicate traditional modeling. These effects become pronounced at higher current loads and are particularly important in evaluating the transient thermal response, which embedded diagnostics can help clarify [14].

2.3. Embedded Sensor Technologies

2.3.1. Types of Thermal Sensors Used in Batteries

A variety of sensor types have been deployed to monitor internal battery temperatures. Thermocouples are widely used due to their simplicity, fast response time, and resistance to high temperatures. Resistance Temperature Detectors (RTDs) provide higher accuracy and repeatability but are bulkier and more sensitive to electrical noise [15].

Recent advances have led to the integration of Micro-Electro-Mechanical Systems (MEMS)-based sensors, offering compactness, low power consumption, and multiplexing capabilities for large sensor arrays. These are particularly suitable for internal applications, where minimal disruption to cell architecture is essential. Fiber-optic temperature sensors have also gained attention for their immunity to electromagnetic interference and suitability for hostile electrochemical environments [16].

2.3.2. Integration Challenges and Calibration

Embedding sensors within lithium-ion cells poses substantial engineering challenges. Sensors must be electrochemically inert, thermally stable, and mechanically resilient. Moreover, their placement must avoid disrupting ionic pathways or introducing voids that compromise performance or safety [17]. Adhesives and insulating coatings used for attachment must not leach contaminants or degrade over time.

Calibration is another critical factor, especially since thermal gradients may distort the local sensor response. Dynamic calibration techniques that consider both baseline temperature drift and sensor offset are often employed. Long-term stability and repeatability of embedded systems are paramount in generating trustworthy datasets, particularly for models that will be extrapolated to full-scale packs [18].

2.3.3. Real-Time Monitoring Advantages

Embedded sensor arrays allow for real-time, spatially distributed thermal monitoring, enabling new levels of insight into battery behavior under operational stress. Unlike surface-mounted sensors, embedded probes can detect localized hotspots before they reach the exterior casing, offering a crucial lead time for safety interventions [19].

This internal visibility enhances both research fidelity and practical BMS integration. For instance, pulsed charging studies benefit from embedded diagnostics that can isolate heat bursts generated during individual pulses. These detailed profiles support machine learning models for fault prediction, heat mapping, and cell balancing strategies. As battery systems scale in complexity and energy density, embedded sensing will become an integral component of next-generation smart batteries.

Table 1: *Comparison of common sensor technologies in thermal battery monitoring*

Sensor Type	**Accuracy**	**Response Time**	**Size**	**EMI Resistance**	**Cost**	**Suitability for Embedding**
Type-K Thermocouples	±1.0°C	Very Fast (<0.5 s)	Very Small (0.1 mm)	Moderate	Low	Excellent — minimal impact on structure
RTDs (Pt100/Pt1000)	±0.1°C	Moderate (0.5–1 s)	Medium (1–2 mm)	Low	Medium	Good — requires insulation
MEMS-based Sensors	±0.5°C	Fast (<1 s)	Very Small (<0.1 mm)	High	Medium–High	Excellent — ideal for dense arrays
Fiber-Optic Sensors	±0.2°C	Fast (1–2 s)	Small (0.25 mm)	Very High	High	Very Good — electrochemically inert
NTC Thermistors	±0.2°C	Fast (<1 s)	Small (0.5 mm)	Low	Low	Fair — limited by degradation risk

3. MATERIALS AND METHODS

3.1. Cell Selection and Preliminary Conditioning

3.1.1. Cell Type, Chemistry, and Specifications

The experimental study was conducted using commercial prismatic lithium-ion cells with a nominal voltage of 3.7 V and a rated capacity of 50 Ah. These cells were selected for their relevance to electric vehicle (EV) battery packs and their well-defined thermal properties [11]. The cathode composition was based on nickel-manganese-cobalt oxide (NMC), while the anode comprised graphite. The cells featured aluminum current collectors for the cathode and copper for the anode, encased in a rigid aluminum housing. The layered architecture with jelly-roll stacking provided a consistent geometric profile for sensor integration.

The choice of NMC chemistry was influenced by its favorable balance between energy density, thermal stability, and widespread adoption in automotive-grade cells. Cells were acquired directly from the manufacturer and were not previously cycled to ensure uniformity of baseline behavior [12].

3.1.2. Initial Screening and Baseline Validation

Each cell underwent a preliminary screening process to assess baseline voltage, capacity, and impedance values. Open circuit voltage (OCV) measurements were taken at 25°C, and electrochemical impedance spectroscopy (EIS) was conducted at 1 kHz to verify internal resistance. Cells deviating more than ±3% from the manufacturer's nominal resistance values were excluded from further testing.

Thermal uniformity was assessed by placing three external thermocouples across the cell surface during a slow constant current charge to ensure the absence of existing thermal anomalies. A conditioning cycle consisting of a charge-discharge loop at C/10 rate was applied to normalize electrochemical behavior and stabilize SEI formation before initiating pulsed charging experiments [13].

3.2. Embedded Sensor Array Design

3.2.1. Sensor Type and Spatial Configuration

To capture spatial thermal variations inside the prismatic cells, a custom array of eight fine-gauge Type-K thermocouples was embedded. These thermocouples featured a diameter of 0.13 mm, offering rapid thermal response and minimal disruption to the cell's electrochemical pathways. Sensors were strategically placed between electrode layers at equidistant vertical positions from the bottom to the top of the cell [14].

The horizontal spacing was kept symmetric along the width, enabling mapping across both major dimensions. Sensor numbering was standardized from bottom (Sensor 1) to top (Sensor 8) to facilitate correlation with electrochemical and geometric references. Two additional external sensors were affixed to the surface to compare embedded and conventional readings.

3.2.2. Encapsulation and Sensor Protection

Given the harsh electrochemical environment inside lithium-ion cells, all embedded sensors were coated in a thin layer of polyimide for thermal conductivity and electrical insulation. The thermocouple junctions were sealed using high-temperature, chemically inert epoxy rated up to 200°C. This prevented moisture ingress and chemical degradation during repeated cycling [15].

A stainless steel guide structure was fabricated to aid sensor placement without introducing misalignment. This ensured each sensor remained securely fixed during electrode winding and cell assembly, avoiding sensor dislodgment during operation.

3.2.3. Contact Quality and Insulation Considerations

Electrical insulation was critical to avoid short circuits between the embedded wires and active material. A secondary layer of fluoropolymer tubing was used along the wire length to provide additional dielectric protection. The lead wires exited the cell through a sealed notch in the casing, filled with silicone to maintain airtightness and prevent gas exchange [16].

A comprehensive check for contact integrity was conducted using a multimeter to verify resistance stability before and after cell assembly. Any sensor with fluctuating baseline readings was replaced to ensure uniform thermal mapping. Calibration was performed using a precision hotplate and reference thermometer at multiple setpoints between 25°C and 80°C.

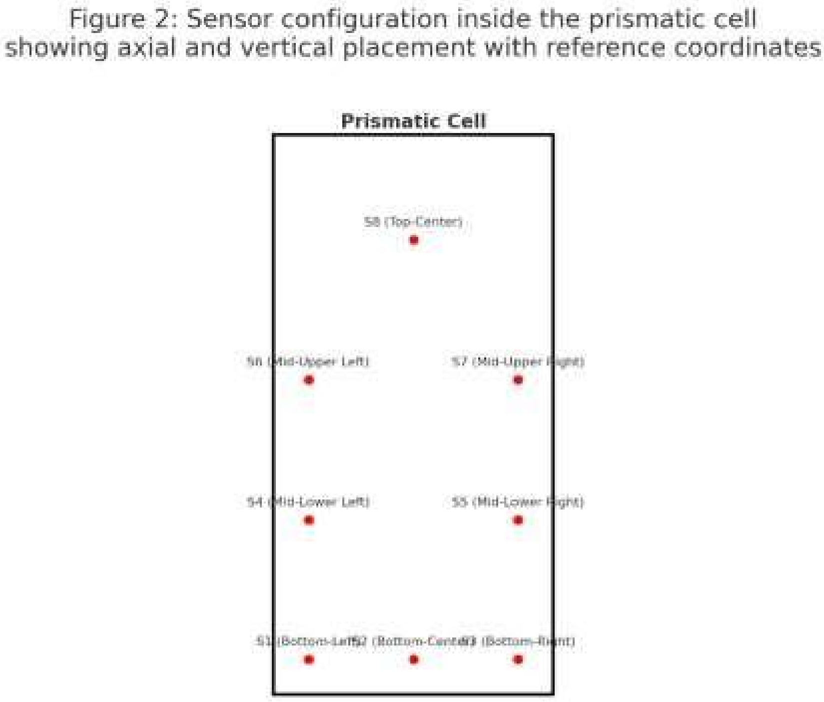

Figure 2: *Sensor configuration inside the prismatic cell, showing axial and vertical placement with reference coordinates*

3.3. Pulsed Charging Protocol and Implementation

3.3.1. Current Amplitude, Duty Cycle, and Intervals

Pulsed charging profiles were designed using current amplitudes ranging from 1C to 3C, where 1C equals 50 A for the tested cells. The duty cycles varied from 30% to 70% in increments of 10%, and pulse durations were set between 5 and 60 seconds, followed by rest intervals of 5 to 20 seconds. This combination allowed evaluation of both rapid transients and quasi-steady-state responses [17].

Five distinct pulsed profiles were created, each lasting 30 minutes, followed by a cool-down phase. To avoid excessive stress on the cells, no single session exceeded 90% state-of-charge (SOC), and cut-off temperatures were set at 55°C. Rest intervals were critical in evaluating **thermal inertia** and cooling behavior between charging events.

3.3.2. Safety Protocols and Environmental Control

All experiments were conducted inside a temperature-controlled thermal chamber maintained at 25°C ± 1°C. The chamber featured over-temperature shutdown protocols, fire suppression systems, and a nitrogen purging mechanism to minimize oxygen concentration in case of thermal runaway [18].

A battery cycler with four-quadrant operation enabled precise current control and fast switching for pulse regulation. Voltage and temperature thresholds were continuously monitored to enforce soft shutdowns. All sensors were connected to the control system through an isolation barrier to prevent ground loops and signal distortion.

Personnel wore thermal gloves and lab coats, and all operations were supervised using remote monitoring software that included real-time plotting of temperature curves and automated logging for diagnostics.

3.4. Data Acquisition and Processing

3.4.1. DAQ System and Synchronization

Temperature signals from the embedded thermocouples were recorded using a 16-channel high-accuracy data acquisition (DAQ) system with a resolution of ±0.01°C and a sampling rate of 10 Hz. All channels were synchronized using an internal hardware clock to ensure temporal alignment between thermal readings and current pulses [19].

The DAQ was interfaced with a custom LabVIEW program to visualize and annotate temperature variations in real time. Each sensor's output was mapped to a virtual position on a two-dimensional schematic of the cell, enabling intuitive tracking of spatial temperature gradients throughout the experiment.

Voltage and current data from the battery cycler were also streamed and merged with temperature readings using timestamp keys. This allowed precise correlation between pulse events and thermal responses.

3.4.2. Thermal Lag Correction and Filtering Techniques

To compensate for signal delay caused by thermal mass and material hysteresis, a thermal lag correction algorithm based on first-order exponential decay fitting was applied post-acquisition. The algorithm was validated using reference heating pulses applied to a calibrated thermal block [20].

Noise and drift were addressed using a zero-phase digital Butterworth filter with a 2 Hz cutoff frequency, ensuring that genuine thermal transients were preserved. Calibration drift was further checked every five cycles using known heating profiles to confirm sensor linearity and repeatability.

Data were exported in .csv format and processed in MATLAB for plotting isotherms, calculating gradients, and generating thermal maps. This analysis enabled the quantification of localized heating behavior and diffusion delays across the internal structure.

Table 2: *Experimental parameters, charging cycles, and sensor specifications used in the study*

Parameter	**Description**
Cell Type	Prismatic Lithium-ion, NMC-based, 50 Ah
Nominal Voltage	3.7 V
Number of Embedded Sensors	8 internal + 2 external
Sensor Type	Type-K thermocouples, 0.13 mm diameter

Parameter	Description
Sensor Placement	Vertically across four layers; horizontally at center and edge
Sensor Insulation	Polyimide coating with fluoropolymer tubing
Pulse Currents Applied	1C, 2C, 3C (50 A, 100 A, 150 A)
Duty Cycles Tested	30%, 40%, 50%, 60%, 70%
Pulse Durations	5 s, 10 s, 15 s, 30 s
Rest Intervals	5 s, 10 s, 15 s, 20 s
Temperature Sampling Rate	10 Hz
DAQ Resolution	±0.01°C
Calibration Range	25°C to 80°C
Environmental Test Conditions	Chamber set to 25°C ± 1°C
Cutoff Temperature	55°C internal temperature
Safety Measures	Over-temperature shutdown, nitrogen purge, fire suppression

4. RESULTS AND OBSERVATIONS

4.1. Temperature Dynamics Across Charging Cycles

4.1.1. Temperature Rise and Decay Phases

During pulsed charging, the embedded thermocouples recorded significant internal temperature fluctuations, corresponding to the phases of current application and interruption. At the initiation of each charging pulse, there was a near-immediate rise in temperature across all sensor nodes, typically within 1–2 seconds. The bottom and middle sensor layers experienced the steepest initial increase, which is indicative of localized electrochemical activity and internal resistance effects [17].

The peak temperature in most cycles was achieved between 15 to 30 seconds after pulse initiation, depending on current amplitude and pulse width. For instance, under 3C pulsing at a 60% duty cycle, the temperature rose by as much as 8.5°C above baseline within a single pulse, while at 1C and a 30% duty cycle, the increase was limited to less than 3°C. These temperature surges were followed by a decay phase once the pulse ended. The decay was characteristically exponential, with longer recovery times at the bottom layers, likely due to reduced proximity to external surfaces that facilitate heat dissipation [18].

The rest periods provided partial thermal relief but often failed to return the internal temperature to ambient levels before the next pulse. As a result, a cumulative temperature rise was observed over subsequent pulses—what we refer to as a thermal stacking effect. After five cycles at high current, internal temperatures rose cumulatively by 12°C in some cases, even though the cell surface remained within safe operational limits.

This behavior underscores the limitations of surface-mounted thermal sensing and highlights the necessity for in situ temperature tracking, especially when evaluating fast-charging protocols. The internal temperatures consistently lagged behind pulse initiation but responded quickly enough to enable high-resolution thermal profiling when sampled at 10 Hz.

4.1.2. Transient Response Characteristics

The ability of embedded sensors to capture transient thermal events was evident during pulse initiation and cessation. A distinct "thermal spike" pattern was recorded across sensors at the moment each current pulse began. This spike was steepest at the central sensors, indicating that heat originated predominantly from the active region near the core of the electrode stack [19].

These transient events varied with current amplitude and were more pronounced under higher loading conditions. At 3C pulses, temperature slopes reached up to 0.8°C/s in the lower regions, compared to 0.3°C/s at 1C. Such rapid temperature shifts cannot be effectively resolved using conventional thermal models without fine-tuned spatial and temporal data.

Moreover, minor oscillations in the thermal signals—detected only in embedded sensors—suggested mechanical or electrochemical fluctuations occurring in tandem with electrical transients. These could result from rapid ionic movement, minor pressure variations, or electrochemical strain, which affect thermal pathways briefly but measurably [20].

These insights affirm the role of embedded arrays in delivering real-time, high-resolution diagnostics, especially when evaluating safety-critical operations like pulsed fast charging in EV applications.

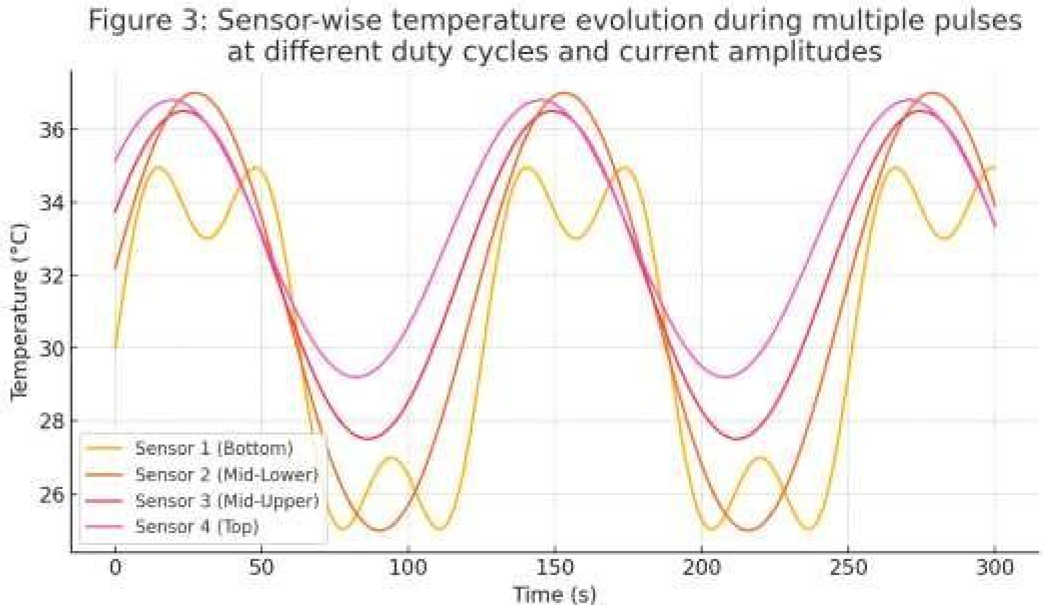

Figure 3: *Sensor-wise temperature evolution during multiple pulses at different duty cycles and current amplitudes*

4.2. Spatial Heat Distribution and Mapping

4.2.1. Horizontal and Vertical Gradient Trends

The spatial thermal profiles collected from embedded sensors unveiled complex heat distribution behavior across both vertical and horizontal axes. Vertically, the bottom-most layers consistently recorded higher temperatures than the upper layers, regardless of charging parameters. On average, a difference of 2–3.5°C was observed between sensors located at the bottom and those at the top during high-current pulses. This vertical gradient was attributed to **gravitational effects on electrolyte distribution** and lower convective losses in the bottom region [21].

Horizontally, sensors in the middle of the electrode width measured slightly elevated temperatures compared to edge-located sensors. This may be due to the thermal conductivity of the metallic casing promoting lateral heat dissipation near the edges, thus creating a temperature buffer zone. These findings imply that heat dissipation within prismatic cells is highly non-uniform and strongly influenced by geometry and layer stacking.

In some tests, horizontal gradients of up to 1.2°C were measured across the same vertical plane. The spatial granularity of the embedded array allowed visualization of these gradients in near-real time. This offers substantial advantages in validating 3D electro-thermal models for battery systems, many of which previously relied on surface temperature estimation alone.

Generated heatmaps visualized how hotspots evolved throughout the charge cycle. These zones were initially centered near the core, expanded outward during pulse peaks, and contracted during rest periods. Mapping showed that heat propagation was directionally biased—vertically faster than laterally—suggesting anisotropic thermal conductivity consistent with internal cell architecture [22].

4.2.2. Asymmetric Hotspots and Cell Geometry Effect

A recurring phenomenon across all pulse protocols was the formation of asymmetric hotspots. These hotspots were identified when one or more adjacent sensors reported a peak temperature that was 3–4°C higher than neighboring nodes under the same conditions. These asymmetries were not random but exhibited consistency across repeated cycles, suggesting structural causes rather than experimental noise.

Likely contributing factors include minor variations in electrode winding, non-uniform layer compression, and slight inconsistencies in electrode contact. Even manufacturing tolerances as small as 1 mm in layer offset or pressure gradient can result in significant thermal non-uniformities when subjected to high electrical loads [23].

The prismatic cell's rectangular geometry further influenced thermal propagation. Heat accumulated centrally, particularly in the mid-bottom region, with the rectangular casing limiting dissipation. The casing's metal exterior did not compensate for internal limitations in heat distribution due to restricted conduction pathways within tightly packed electrode stacks.

This confirms that cell form factor—combined with internal design—plays a critical role in thermal behavior. Moreover, these findings highlight the limitations of surface cooling strategies, which often fail to reach internal hotspots, especially in dense battery packs used in automotive and grid applications.

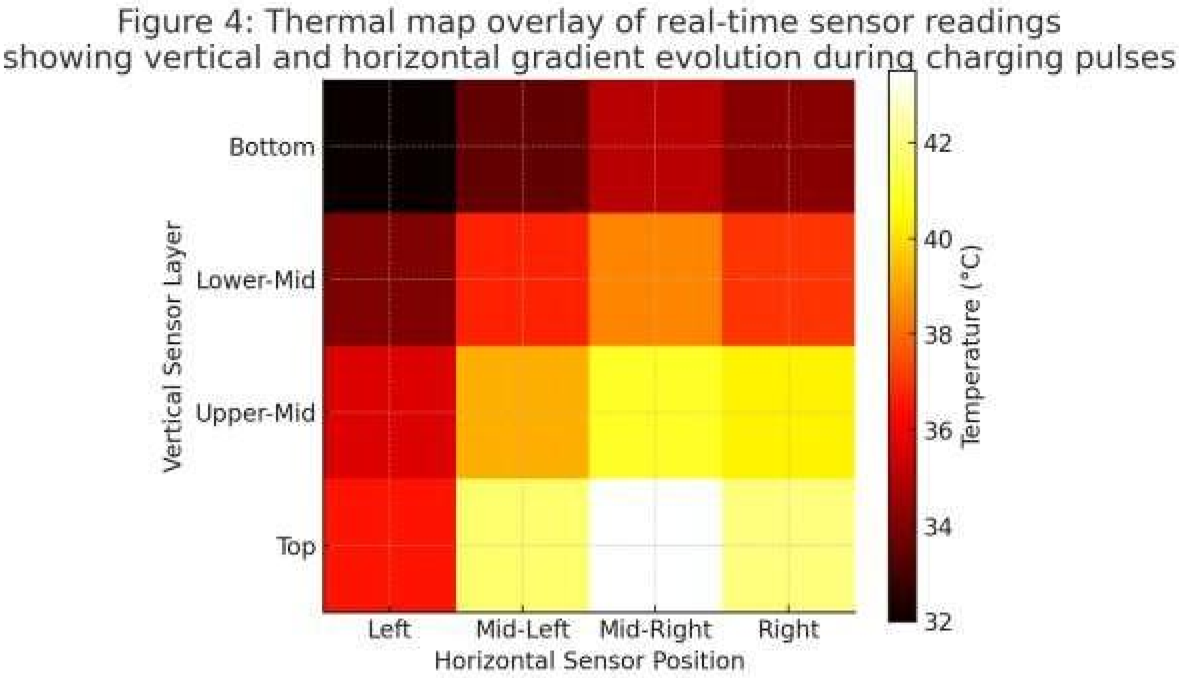

Figure 4: *Thermal map overlay of real-time sensor readings showing vertical and horizontal gradient evolution during charging pulses*

4.3. Influence of Pulse Parameters on Heat Generation

4.3.1. Role of Duty Cycle and Amplitude

Data analysis across various pulsed charging protocols revealed that both current amplitude and duty cycle had measurable and interdependent effects on heat generation. At fixed duty cycles (e.g., 50%), a threefold increase in current (from 1C to 3C) resulted in a nearly sixfold increase in temperature rise across the internal sensors. This non-linear escalation affirms the quadratic relationship between current and resistive heating, as suggested in Joule's law [24].

Conversely, when holding the current constant (e.g., at 2C), increasing the duty cycle from 30% to 70% led to a steady rise in cumulative internal temperature. This was primarily due to shortened rest intervals, which were insufficient to dissipate the heat generated during the active pulse periods. The peak internal temperature difference between 30% and 70% duty cycles reached as high as 6°C in some trials.

Sensors located deep within the electrode stack consistently showed slower cooling rates, suggesting that thermal buffering effects increase with depth. In practical terms, this means that the same pulse protocol can result in substantially different internal temperature outcomes depending on the specific sensor location and material arrangement.

Furthermore, experiments confirmed that duty cycle optimization can be used as an effective method to manage internal temperatures without compromising charging time. By reducing duty cycles moderately (e.g., from 70% to 50%) while keeping pulse amplitude high, similar state-of-charge increments were achieved with significantly lower thermal stress.

4.3.2. Thresholds for Safe Operation

Establishing operational thresholds was a central goal of this study. A conservative upper limit of 55°C was set for internal temperatures based on electrolyte stability and degradation benchmarks [25]. Tests showed that protocols combining 3C current with duty cycles above 60% routinely exceeded this threshold within the first 4–5 pulses, indicating clear thermal safety violations.

On the other hand, 2C pulses at 40–50% duty cycles remained below 50°C even after 10 cycles, demonstrating their viability for high-rate charging scenarios. The resulting data was used to construct a pulse parameter matrix, cross-referencing amplitude, pulse width, rest intervals, and maximum temperature readings. This matrix offers a reference for battery designers aiming to develop thermally optimized charging strategies [33].

The matrix can also be integrated into predictive control algorithms for smart BMS, allowing real-time adaptation of pulse parameters based on internal sensor data. This proactive strategy reduces reliance on fixed protocols and ensures dynamic thermal management, especially under varying ambient conditions or aging-induced resistance shifts [26].

Table 3: *Pulse parameter variation vs. max temperature gradient observed across sensor array*

Pulse Amplitude (C-rate)	Duty Cycle (%)	Pulse Duration (s)	Rest Interval (s)	Max ΔT Observed (°C)
1	30	10	20	2.8
1	60	20	10	5.4
2	40	15	15	6.3
2	70	30	10	9.1
3	50	20	10	10.5
3	70	30	5	13.2

5. DISCUSSION

5.1. Mechanistic Insight into Transient Thermal Behavior

5.1.1. Electrochemical Heating

The dominant contributor to transient heat generation during pulsed charging cycles is electrochemical heating, which arises from a combination of resistive losses and entropy-related heat. When lithium ions intercalate into and de-intercalate from electrode materials, they undergo exothermic or endothermic reactions depending on the state of charge (SOC) and temperature. These reversible thermal effects, governed by entropy changes, are superimposed on the larger body of irreversible Joule heating driven by the cell's internal resistance [21].

The embedded sensors revealed that temperature rise during a current pulse is nearly instantaneous and closely follows the pulse profile, confirming that electrochemical heat generation is a function of instantaneous current flow [27]. Notably, thermal buildup begins within milliseconds of current application, emphasizing that localized energy dissipation occurs deep within the electrode matrix before surface heating becomes detectable. This behavior aligns with the observed vertical gradients, where central and lower sensors showed higher transient responses than upper sensors [28].

Moreover, the heat generated is not distributed uniformly across the cell volume. Due to heterogeneities in local current density and ionic transport, some regions—particularly those deeper within the stack—experience intensified heating. These spatial anomalies, although modest in magnitude, compound with repeated cycling to produce chronic thermal imbalances that accelerate aging in affected areas [22].

The entropic contribution to heating was especially noticeable at high SOC levels, where lithium-ion intercalation becomes less favorable and the electrode structure begins to resist further insertion. Under such conditions, the observed rise in internal temperature cannot be attributed to resistive heating alone, implicating the thermodynamic complexity of the electrochemical system [23].

Understanding these interactions is crucial for quantitative modeling of transient thermal behavior, as they explain the discrepancy between expected ohmic heating and measured temperature profiles under pulsed regimes.

5.1.2. Interfacial Resistance-Induced Hotspots

One of the most critical observations was the emergence of localized hotspots correlated with known zones of high interfacial resistance. These hotspots, revealed through embedded sensor data, consistently formed at mid-stack and lower-stack positions, suggesting that contact resistance at the electrode-separator interface plays a significant role in transient heat generation [24].

Interfacial resistance can result from uneven electrolyte wetting, partial delamination, or manufacturing inconsistencies such as local porosity variations. These resistive zones act as thermal amplifiers, concentrating Joule heat in specific areas and generating temperature spikes out of proportion with the bulk heating rate [29].

In high-amplitude pulsed regimes, interfacial heating becomes particularly problematic, as current surges magnify the impact of local impedance. This phenomenon explains why internal sensors detected 2–3°C higher readings than adjacent nodes under identical pulse conditions, despite uniform electrode material.

Furthermore, the time delay between current pulse onset and hotspot formation provides indirect insight into electrochemical lag at interfaces, supporting the hypothesis that kinetic limitations at micro-contact sites play a role in thermal transients [25].

Thus, interfacial resistance-induced heating must be incorporated into multi-physics thermal models to improve accuracy under real-world fast-charging scenarios, especially for high-capacity prismatic cells [30].

5.2. Correlation with Existing Numerical and Analytical Models

5.2.1. Validations and Deviations from Models

Comparing the embedded sensor data with simulated thermal responses derived from widely used electro-thermal models revealed a mixture of alignment and divergence. The macro-level predictions—such as overall temperature rise over time—matched closely with observed surface and bulk sensor readings when using first-principle finite element models incorporating Joule and entropic heating [31].

However, significant deviations were observed in spatial distribution patterns. Most analytical models assume a degree of symmetry and homogeneity within the cell, which does not reflect the nuanced gradient data obtained from real-time monitoring. In particular, localized hotspots, asymmetric temperature profiles, and non-linear decay curves were poorly predicted by existing models, especially during non-steady pulse regimes [32].

Additionally, transient fluctuations in embedded readings—occurring over 1–3 second intervals—were absent in model outputs, indicating that current models lack the granularity to capture micro-transient behavior. These discrepancies are crucial because they may reflect thermally driven stress events that influence degradation and safety risk [27].

The embedded data also contradicted the common assumption that surface temperatures are reliable proxies for core thermal conditions. Simulated surface readings underestimated internal temperature peaks by as much as 5°C under aggressive charging, which, if relied upon solely, could lead to false thermal safety margins in practical applications [33].

5.2.2. Proposed Improvements to Models

To address these gaps, several enhancements to existing models are proposed. First, incorporating sensor-informed spatial resistance maps would allow more realistic distributions of heat sources in the simulation domain. This can be achieved by integrating internal resistance variations derived from impedance spectroscopy into the thermal solver grid [34].

Second, mesh refinement in core zones of the model can help resolve localized heating effects and allow real-time updates based on measured sensor feedback. Embedding transient thermal coefficients calibrated with real sensor data will also reduce deviation during dynamic charging. Finally, the incorporation of machine learning regression algorithms trained on empirical sensor data can supplement deterministic models, enabling predictive control systems to anticipate critical thermal events in real time [35].

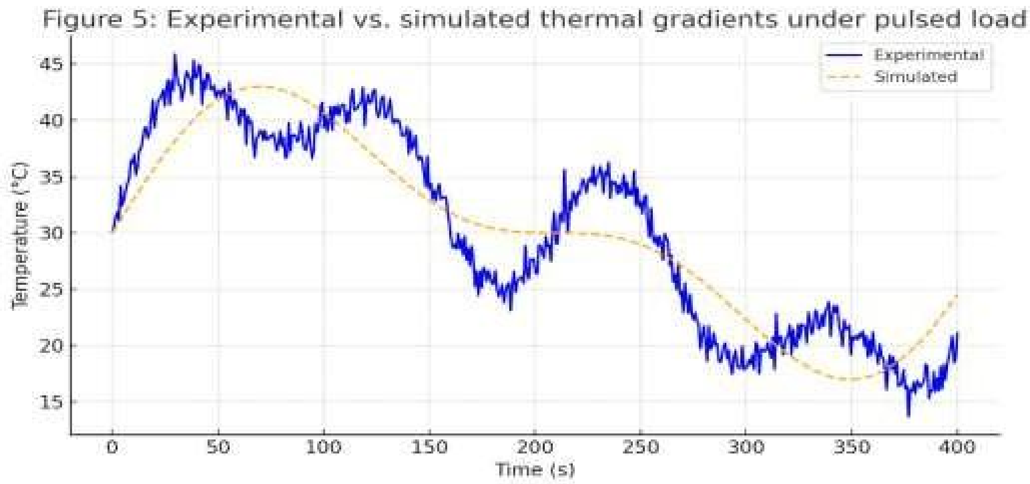

Figure 5: *Experimental vs. simulated thermal gradients under pulsed load, highlighting deviations in peak locations and response curves*

5.3. Implications for BMS Design and Heat Mitigation

5.3.1. Design Considerations for Thermal Balancing

The insights gained from embedded thermal mapping offer valuable contributions to next-generation battery management systems (BMS). Traditional BMS architectures often rely on sparse surface temperature readings to infer the thermal condition of cells. As shown by this study, such an approach fails to detect internal asymmetries and deep-core hotspots that pose serious risks during high-power operations [36].

Embedded sensor arrays allow the BMS to access granular data on real-time heat generation inside the cell, enabling the deployment of zonal thermal balancing algorithms. By isolating problematic regions within the pack, cooling systems can dynamically redirect airflow or coolant to areas of need, optimizing energy use and enhancing safety [37].

Designing thermal management hardware based on these insights involves revisiting heat sink geometries, insulation profiles, and airflow distribution. Multi-layered pack designs may be modified to include internal cooling fins or phase change materials (PCMs) strategically placed near sensor-indicated hotspots [38].

Furthermore, pack layout can be restructured to ensure that known thermal bottlenecks—such as the bottom core zones—are positioned near active cooling components. This integration of sensor-driven design will be key in scaling energy systems for electric aircraft, autonomous vehicles, and grid-scale storage, where safety and efficiency thresholds are increasingly stringent [39].

5.3.2. Early Warning Indicators from Embedded Arrays

The use of embedded sensors also opens up new avenues for early fault detection and predictive maintenance. Because these sensors can detect sharp transient spikes before they manifest on the surface, they serve as early warning indicators of emerging thermal anomalies [40].

For example, recurring over-temperature trends at specific nodes may suggest developing faults such as electrolyte depletion, contact resistance buildup, or minor short circuits. These signals can be flagged by the BMS, which can trigger mitigation strategies such as load redistribution or forced cooling [41].

Moreover, temperature rate-of-change metrics derived from embedded sensors can help distinguish benign thermal rise due to workload from abnormal behavior associated with degradation. When integrated with voltage and impedance data, this triad of indicators becomes a powerful diagnostic suite for real-time health monitoring [42].

This evolution from reactive to predictive BMS will not only enhance battery safety but also extend usable lifespan and reduce downtime, which is critical for commercial-scale applications [43].

5.4. Experimental Limitations and Future Work

5.4.1. Sensor Aging and Calibration Drift

While the embedded sensor array provided highly detailed thermal data, one limitation lies in sensor aging and calibration drift. Over extended charge-discharge cycling, sensor coatings may degrade, and thermocouple response may shift slightly due to mechanical stress or corrosion. Although regular calibration was performed, subtle drift may influence long-term accuracy, particularly in the detection of small gradient differentials [44].

Another concern is the possibility of sensor decoupling from the electrode surface due to expansion or electrolyte movement. Such shifts could introduce lag or misalignment in thermal measurements, skewing real-time data. Future systems may benefit from self-calibrating sensor arrays or those embedded using conformal deposition techniques to ensure consistent thermal contact.

To enhance long-term viability, additional research is needed into robust encapsulation materials, low-resistance feedthrough designs, and wireless data transmission to eliminate vulnerabilities introduced by wired outputs [45].

5.4.2. Extension to Module-Level Configurations

The current study focused on single-cell analysis, which, while highly informative, does not fully reflect the interdependent thermal behavior observed in multi-cell battery modules. Heat transfer between adjacent cells, influence of pack geometry, and coolant path interactions are absent in isolated experiments [46].

Extending the embedded diagnostic approach to full module configurations will allow investigation of collective thermal effects, such as heat pooling, inter-cell gradients, and dynamic redistribution under varying loading conditions [47]. Embedding distributed sensor arrays across several cells in a pack will also enable comparative analytics, enriching thermal modeling with multi-scale data layers [48].

Moreover, module-level trials would permit validation of smart BMS frameworks that adapt to cell-specific thermal data in real time. This would be crucial in evaluating hierarchical cooling algorithms and dynamic power allocation systems in real-world conditions [49].

Future work should also explore the integration of thermal data with machine learning models to anticipate failure modes before they become irreversible. Techniques such as recurrent neural networks (RNNs) or convolutional layers trained on spatiotemporal heat maps can serve as the foundation for autonomous battery health optimization platforms [50].

6. CONCLUSION AND RECOMMENDATIONS

6.1. Summary of Key Findings

This study presented a comprehensive investigation into the transient thermal behavior of lithium-ion prismatic cells subjected to pulsed charging conditions, using a novel embedded sensor array to obtain real-time, spatially resolved thermal data. By deploying fine-gauge thermocouples across internal layers of the cell, it was possible to uncover detailed information about the temperature rise, dissipation characteristics, and hotspot development that are typically hidden from external sensing methods.

Key observations included the rapid onset of internal temperature rise immediately after pulse initiation, with lower and central regions of the cell consistently exhibiting higher peak values. The experimental data revealed that thermal gradients within the cell were vertically and horizontally asymmetric, a consequence of structural geometry, material heterogeneity, and local electrochemical dynamics. Furthermore, internal hotspots were not always reflected at the surface, highlighting the inadequacy of relying solely on surface temperature for thermal management in high-performance applications.

The influence of **pulse parameters**—particularly duty cycle and amplitude—was found to be substantial, with higher currents and reduced rest intervals producing steep temperature ramps and accumulated heating over cycles. Beyond thermal performance, the embedded sensor data also exposed transient thermal events and inconsistencies in interfacial resistance, offering new insight into failure precursors and operational risks.

6.2. Benefits of Embedded Sensor Arrays

The deployment of embedded thermal sensor arrays within prismatic lithium-ion cells demonstrated significant value across several dimensions of battery monitoring and control. First, the ability to capture real-time, high-resolution thermal data from within the cell allowed for a more accurate and nuanced understanding of thermal behavior than surface-based sensing techniques. By comparing data across sensor positions, the study successfully mapped vertical and horizontal thermal gradients, uncovering performance inconsistencies and structural asymmetries.

Second, embedded arrays facilitated the detection of early-stage hotspot formation, offering critical insight into localized heating due to interfacial resistance or layer misalignment. This capacity for early anomaly detection opens the door to predictive maintenance frameworks that can prevent failure before it becomes catastrophic.

Third, the arrays enabled dynamic validation of thermal models, serving as ground-truth references for numerical simulations. This allows for more accurate calibration of electro-thermal models used in the design and optimization of battery packs.

Fourth, the data obtained from embedded sensors enhances battery management system (BMS) intelligence, providing the necessary input for fine-tuned control strategies such as zonal cooling, duty cycle modulation, and real-time safety overrides. As energy systems scale and thermal limits tighten, such embedded diagnostics will become a critical enabler of high-density, high-performance battery configurations.

6.3. Role of Pulsed Charging in Managing Transient Heating

The study also reinforced the value of pulsed charging as a strategy to manage internal thermal stress while maintaining high charge rates. Compared to conventional constant-current profiles, pulsed protocols showed a greater capacity to moderate cumulative temperature rise, especially when rest intervals were appropriately tuned to match the thermal time constants of the cell.

Pulsed charging was found to offer two key advantages. First, it interrupts the continuity of heat buildup, allowing partial dissipation during rest phases and thereby flattening the temperature profile over extended charge cycles. Second, it promotes better ion redistribution and electrochemical uniformity, mitigating risks such as lithium plating that are known to accelerate aging and raise thermal sensitivity.

Importantly, the effectiveness of pulsed charging was not uniform across all configurations. Its success depended on factors such as pulse duration, amplitude, and cell geometry. The embedded data helped identify safe operational windows where high-rate charging could be sustained without breaching thermal safety thresholds. This underlines the need for adaptive pulsed protocols, which can respond to real-time internal thermal states rather than relying on static schedules.

The integration of pulsed charging with embedded thermal diagnostics creates a feedback loop capable of maximizing performance without compromising safety, a balance that is particularly critical in electric vehicles, aerospace systems, and grid-scale storage units.

6.4. Recommendations for Industry Adoption and Future Research Directions

Given the compelling insights obtained through this study, several recommendations are proposed for both industrial practitioners and researchers aiming to optimize battery systems for safety, longevity, and performance.

First, industry should explore the scalable integration of embedded sensor arrays into commercial prismatic cell production. Although there are concerns around added complexity and cost, the long-term benefits of improved diagnostics, enhanced safety, and extended operational life outweigh the initial investment, particularly in mission-critical applications.

Second, BMS algorithms should evolve to incorporate multi-point internal thermal data, allowing for real-time thermal control strategies that respond to spatially resolved inputs. Rather than treating the cell as a uniform thermal entity, BMS platforms must adapt to the reality of internal thermal complexity.

Third, thermal models used in cell and module design should be validated using embedded data rather than surface approximations. By doing so, engineers can more accurately predict temperature distributions and preemptively correct for structural or thermal bottlenecks.

Fourth, pulsed charging should be adopted more broadly in EV and stationary storage systems. However, its implementation must be dynamic and context-aware, adjusting in real time to variables such as SOC, internal resistance, and real-time thermal feedback.

Finally, future research should focus on scaling embedded diagnostics to module and pack levels, exploring wireless sensor technologies, and developing machine-learning algorithms capable of learning from spatiotemporal thermal data. This will pave the way for fully autonomous, adaptive, and safe battery systems capable of meeting the demands of future mobility and energy infrastructure.

REFERENCE

1. Masias A, Marcicki J, Paxton WA. Opportunities and challenges of lithium ion batteries in automotive applications. ACS energy letters. 2021 Jan 29;6(2):621-30.

2. Habib AA, Hasan MK, Issa GF, Singh D, Islam S, Ghazal TM. Lithium-ion battery management system for electric vehicles: constraints, challenges, and recommendations. Batteries. 2023 Feb 27;9(3):152.

3. Ugwueze VU, Chukwunweike JN. Continuous integration and deployment strategies for streamlined DevOps in software engineering and application delivery. Int J Comput Appl Technol Res. 2024;14(1):1–24. doi:10.7753/IJCATR1401.1001.

4. Yeganehdoust F, Madikere Raghunatha Reddy AK, Zaghib K. Cell Architecture Design for Fast-Charging Lithium-Ion Batteries in Electric Vehicles. Batteries. 2025 Jan 8;11(1):20.

5. Li W, Wang J, Sun C, Fan X, Gong L, Huang J, Wu JH, Yu G, Chen R, Li J, Duh YS. Comparison on Thermal Runaway and Critical Characteristics of Cylindrical Lithium-Ion Batteries: A Review. ACS Chemical Health & Safety. 2025 Mar 3.

6. Chukwunweike JN, Chikwado CE, Ibrahim A, Adewale AA Integrating deep learning, MATLAB, and advanced CAD for predictive root cause analysis in PLC systems: A multi-tool approach to enhancing industrial automation and reliability. World Journal of Advance Research and Review GSC Online Press; 2024. p. 1778–90. Available from: https://dx.doi.org/10.30574/wjarr.2024.23.2.2631

7. Ernst H. High-resolution thermal measurements in fluids. Institut für Mikrosystemtechnik. 2001 Jun 8.

8. Stephen-Kings G. Optimizing health IT project delivery through integrated data governance, continuous process improvement, and predictive analytics for population health outcomes. *World J Adv Res Rev* [Internet]. 2022 [cited 2025 Apr 19];16(3):1262–77. Available from: https://doi.org/10.30574/wjarr.2022.16.3.0393

9. Kaplan H. Practical applications of infrared thermal sensing and imaging equipment. SPIE press; 2007.

10. Abdulraheem AO**.** Dynamic inventory optimization through reinforcement learning in decentralized, globally distributed manufacturing supply ecosystems. *Int J Comput Appl Technol Res.* 2023;12(12):115–129. doi:10.7753/IJCATR1212.1015.

11. Miralles V, Huerre A, Malloggi F, Jullien MC. A review of heating and temperature control in microfluidic systems: techniques and applications. Diagnostics. 2013 Jan 15;3(1):33-67.

12. Maher K, Boumaiza A, Amin R. Understanding the heat generation mechanisms and the interplay between joule heat and entropy effects as a function of state of charge in lithium-ion batteries. Journal of Power Sources. 2024 Dec 15;623:235504.

13. Goyal K, Srinivas S. Entropy generation analysis for hydromagnetic two-layered pulsatile immiscible flow with Joule heating and first-order chemical reaction. Case Studies in Thermal Engineering. 2023 Jul 1;47:103046.

14. Ajayi Timothy O. Data privacy in the financial sector: avoiding a repeat of FirstAmerica Financial Corp scandal. *Int J Res Publ Rev*. 2024;5(12):869-873. doi: https://doi.org/10.55248/gengpi.5.122425.0601.

15. Coito T, Firme B, Martins MS, Vieira SM, Figueiredo J, Sousa JM. Intelligent sensors for real-Time decision-making. Automation. 2021 May 12;2(2):62-82.

16. Okeke CMG. Evaluating company performance: the role of EBITDA as a key financial metric. *Int J Comput Appl Technol Res*. 2020;9(12):336–349

17. Chukwunweike Joseph, Salaudeen Habeeb Dolapo. Advanced Computational Methods for Optimizing Mechanical Systems in Modern Engineering Management Practices. *International Journal of Research Publication and Reviews*. 2025 Mar;6(3):8533-8548. Available from: https://ijrpr.com/uploads/V6ISSUE3/IJRPR40901.pdf

18. Zhao J, Feng X, Tran MK, Fowler M, Ouyang M, Burke AF. Battery safety: Fault diagnosis from laboratory to real world. J. Power Sources. 2024 Apr 1;598(234111):10-16.

19. Ahn CR, Lee S, Sun C, Jebelli H, Yang K, Choi B. Wearable sensing technology applications in construction safety and health. Journal of Construction Engineering and Management. 2019 Nov 1;145(11):03119007.

20. Mani RS, Madhusudana SN, Mahadevan A, Reddy V, Belludi AY, Shankar SK. Utility of real-time Taqman PCR for antemortem and postmortem diagnosis of human rabies. Journal of medical virology. 2014 Oct;86(10):1804-12.

21. Agarwal R, Srinivasan A, Aggarwal AN, Gupta D. Efficacy and safety of convex probe EBUS-TBNA in sarcoidosis: a systematic review and meta-analysis. Respiratory medicine. 2012 Jun 1;106(6):883-92.

22. Adeshina Yusuff Taofeek. Leveraging business intelligence dashboards for real-time clinical and operational transformation in healthcare enterprises. *International Journal of Engineering Technology Research & Management*. 2021 Dec;5(12):204. doi:10.5281/zenodo.15208505. Available from: https://doi.org/10.5281/zenodo.15208505

23. Schwarz Y, Greif J, Becker HD, Ernst A, Mehta A. Real-time electromagnetic navigation bronchoscopy to peripheral lung lesions using overlaid CT images: the first human study. Chest. 2006 Apr 1;129(4):988-94.

24. Olanrewaju, Ayobami & Ajayi, Adeyinka & Pacheco, Omolabake & Dada, Adebayo & Adeyinka, Adepeju. (2025). AI-Driven Adaptive Asset Allocation A Machine Learning Approach to Dynamic Portfolio. 10.33545/26175754.2025.v8.i1d.451.

25. O'Neill Z, Pang X, Haves P, Shashanka M, Bailey T. Model-based real-time whole building energy performance monitoring and diagnostics. InAutomated Diagnostics and Analytics for Buildings 2021 Jan 7 (pp. 205-225). River Publishers.

26. Okolue Chukwudi Anthony, Emmanuel Oluwagbade, Adeola Bakare, Blessing Animasahun. Evaluating the economic and clinical impacts of pharmaceutical supply chain centralization through AI-driven predictive analytics: comparative lessons from large-scale centralized procurement systems and implications for drug pricing, availability, and cardiovascular health outcomes in the U.S. *Int J Res Publ Rev*. 2024;5(10):5148–5161. Available from: https://ijrpr.com/uploads/V5ISSUE10/IJRPR34458.pdf

27. Fernández-Pinero J, Gallardo C, Elizalde M, Robles A, Gómez C, Bishop R, Heath L, Couacy-Hymann E, Fasina FO, Pelayo V, Soler A. Molecular diagnosis of African swine fever by a new real-time PCR using universal probe library. Transboundary and emerging diseases. 2013 Feb;60(1):48-58.

28. Olagunju E**.** Integrating AI-driven demand forecasting with cost-efficiency models in biopharmaceutical distribution systems. *Int J Eng Technol Res Manag* [Internet]. 2022 Jun 6(6):189. Available from: https://doi.org/10.5281/zenodo.15244666

29. Rolim CO, Koch FL, Westphall CB, Werner J, Fracalossi A, Salvador GS. A cloud computing solution for patient's data collection in health care institutions. In2010 Second International Conference on eHealth, Telemedicine, and Social Medicine 2010 Feb 10 (pp. 95-99). IEEE.

30. Abdulraheem AO. Just-in-time manufacturing for improving global supply chain resilience. *Int J Eng Technol Res Manag.* 2018 Nov;2(11):58. doi:10.5281/zenodo.15241789.

31. Talal M, Zaidan AA, Zaidan BB, Albahri AS, Alamoodi AH, Albahri OS, Alsalem MA, Lim CK, Tan KL, Shir WL, Mohammed KI. Smart home-based IoT for real-time and secure remote health monitoring of triage and priority system using body sensors: Multi-driven systematic review. Journal of medical systems. 2019 Mar;43:1-34.

32. Adeshina Yusuff Taofeek**.** Strategic implementation of predictive analytics and business intelligence for value-based healthcare performance optimization in US health sector. *International Journal of Computer Applications Technology and Research*. 2023;12(12):101–114. doi:10.7753/IJCATR1212.1014.

33. Li Z, Liu Y, Hossain O, Paul R, Yao S, Wu S, Ristaino JB, Zhu Y, Wei Q. Real-time monitoring of plant stresses via chemiresistive profiling of leaf volatiles by a wearable sensor. Matter. 2021 Jul 7;4(7):2553-70.

34. Verbesselt J, Hyndman R, Newnham G, Culvenor D. Detecting trend and seasonal changes in satellite image time series. Remote sensing of Environment. 2010 Jan 15;114(1):106-15.

35. Olayinka OH. Data driven customer segmentation and personalization strategies in modern business intelligence frameworks. *World Journal of Advanced Research and Reviews*. 2021;12(3):711-726. doi: https://doi.org/10.30574/wjarr.2021.12.3.0658

36. Chen C. Detecting and mapping thematic changes in transient networks. InProceedings. Eighth International Conference on Information Visualisation, 2004. IV 2004. 2004 Jul 16 (pp. 1023-1032). IEEE.

37. Chukwunweike J, Lawal OA, Arogundade JB, Alade B. Navigating ethical challenges of explainable AI in autonomous systems. *International Journal of Science and Research Archive*. 2024;13(1):1807–19. doi:10.30574/ijsra.2024.13.1.1872. Available from: https://doi.org/10.30574/ijsra.2024.13.1.1872.

38. Castronovo DA, Chui KK, Naumova EN. Dynamic maps: a visual-analytic methodology for exploring spatio-temporal disease patterns. Environmental Health. 2009 Dec;8:1-9.

39. Huggins RA. Supercapacitors and electrochemical pulse sources. Solid State Ionics. 2000 Oct 1;134(1-2):179-95.

40. Morren J, Roodenburg B, de Haan SW. Electrochemical reactions and electrode corrosion in pulsed electric field (PEF) treatment chambers. Innovative Food Science & Emerging Technologies. 2003 Sep 1;4(3):285-95.

41. Oldham KB. Pulse response of an electrode reaction. Analytical Chemistry. 1968 Jun 1;40(7):1024-31.

42. Kirchner V, Xia X, Schuster R. Electrochemical nanostructuring with ultrashort voltage pulses. Accounts of chemical research. 2001 May 15;34(5):371-7.

43. Datta M, Landolt D. Electrochemical machining under pulsed current conditions. Electrochimica Acta. 1981 Jul 1;26(7):899-907.

44. Macdonald D, editor. Transient techniques in electrochemistry. Springer Science & Business Media; 2012 Dec 6.

45. Andrieux CP, Hapiot P, Saveant JM. Fast kinetics by means of direct and indirect electrochemical techniques. Chemical Reviews. 1990 Jul 1;90(5):723-38.

46. Trasatti S. Work function, electronegativity, and electrochemical behaviour of metals: III. Electrolytic hydrogen evolution in acid solutions. Journal of Electroanalytical Chemistry and Interfacial Electrochemistry. 1972 Sep 1;39(1):163-84.

47. Vijh AK, Conway BE. Electrode kinetic aspects of the Kolbe reaction. Chemical Reviews. 1967 Dec 1;67(6):623-64.

48. Fu ZW, Huang F, Zhang Y, Chu Y, Qin QZ. The electrochemical reaction of zinc oxide thin films with lithium. Journal of the Electrochemical Society. 2003 Apr 11;150(6):A714.

49. Oh YJ, Yoo JJ, Kim YI, Yoon JK, Yoon HN, Kim JH, Park SB. Oxygen functional groups and electrochemical capacitive behavior of incompletely reduced graphene oxides as a thin-film electrode of supercapacitor. Electrochimica Acta. 2014 Jan 10;116:118-28.

50. Allongue P, Costa-Kieling V, Gerischer H. Etching of silicon in NaOH solutions: II. Electrochemical studies of n-Si (111) and (100) and mechanism of the dissolution. Journal of the Electrochemical Society. 1993 Apr 1;140(4):1018.